Chapter 35
Later Phases of Core Evolution

35.1 Nuclear Cycles

The stellar evolution described above may seem to be rather complicated with regard to the nuclear shell instabilities, but also where the changes of the surface layers are concerned, for example, in the case of evolutionary tracks in the HR diagram. The processes appear much simpler and even become qualitatively predictable if we concentrate only on the central evolution. Extrapolating from central hydrogen and helium burning of sufficiently massive stars, we can imagine that the central region continues to pass through cycles of nuclear evolution which are represented by the following simple scheme:

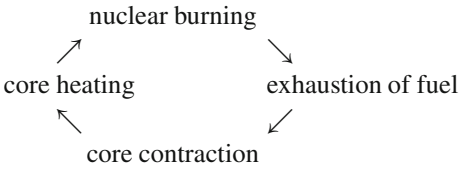

The momentary burning will gradually consume all nuclei inside the convective core that serve as "fuel". The exhausted core then contracts. This raises the central temperature until the next higher burning is ignited etc.

As long as this scheme works, gradually heavier elements are built up near the centre from cycle to cycle. The new elements are evenly distributed in convective cores which usually become smaller with each step. For example, in the first cycle (hydrogen burning), the star develops a massive helium core, inside which a much smaller CO core is produced in the next cycle (helium burning), and so on.

We have also seen that after the core is exhausted the burning usually continues in a concentric shell at the hottest place where the fuel is still present. A shell source can survive several of the succeeding nuclear cycles, each of which generates a new shell source, such that several of them can simultaneously burn outwards through

R. Kippenhahn et al., *Stellar Structure and Evolution*, Astronomy and Astrophysics Library, DOI 10.1007/978-3-642-30304-3_35, © Springer-Verlag Berlin Heidelberg 2012

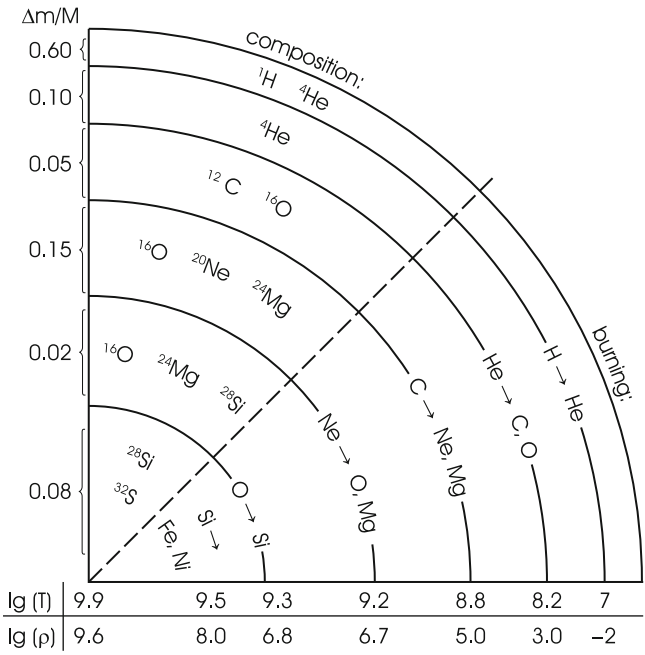

Fig. 35.1 Schematic illustration (not to scale) of the "onion skin structure" in the interior of a highly evolved massive star. Along the vertical radius and below the horizontal radius some typical values of the mass, the temperature (in K), and the density (in g cm^{-3}) are indicated

the star. They are separated by mass shells of different chemical composition; gradually heavier elements are encountered when going inwards from shell to shell. One then speaks of an "onion skin model". A schematical cross section of such a model is shown in Fig. 35.1. The shell structure of the chemical composition can in fact become more complicated than that, since some shell sources bring forth a convective (or semiconvective) subshell, inside which the newly processed material is completely (or partially) mixed. This can be recognized in Fig. 36.4, which shows the interior composition of a model for a $25M_{\odot}$ star in a very advanced stage (just before core collapse, see Chap. 36). We have also seen that, depending on the change of T in certain regions, a shell source may stop burning for some time and be reignited later.

The simple evolution through nuclear cycles as sketched above can obviously be interrupted, either temporarily or for good. From the discussion of the nuclear reactions in Chap. 18 we know that the cycles must come to a termination, at the latest, when the innermost core consists of ^{56}Fe (or neighbouring nuclei) and no further exothermic fusions are possible. However, it is easily seen that the sequence of cycles can be interrupted much earlier by another effect. Each contraction between consecutive burnings increases the central density ϱ_c. Assuming homology

for the contracting core (cf. Sect. 28.1) and ignoring the influence of the rest of the star, we obtain from (28.1) the change of the central temperature T_c

$$\frac{dT_c}{T_c} = \left(\frac{4\alpha - 3}{3\delta}\right) \frac{d\varrho_c}{\varrho_c}. \tag{35.1}$$

The decisive factor, in parenthesis on the right-hand side, depends critically on the equation of state which is written as $\varrho \sim P^\alpha T^{-\delta}$. For an ideal gas with $\alpha = \delta = 1$, we have $dT_c/T_c = (1/3)(d\varrho_c/\varrho_c)$. This means that each contraction of the central region increases the temperature, as well as the degeneracy parameter ψ of the electron gas [ψ = constant for $dT/T = (2/3)(d\varrho/\varrho)$ (cf. Sects. 15.4 and 16.2)]. With increasing degeneracy the exponents α and δ become smaller. When the critical value $\alpha = 3/4$ is reached (δ is then still > 0), the contraction ($d\varrho_c > 0$) no longer leads to a further increase of T_c according to (35.1). The degeneracy in the central region has obviously decoupled the thermal from the mechanical evolution, and the cycle of consecutive nuclear burnings is interrupted. In this case the next burning can be ignited only via more complicated secondary effects, which originate, for example, in the evolution of the surrounding shell source (cf. Sect. 33.2).

Other complications may arise if the central region of a star suffers an appreciable loss of energy by strong neutrino emission (cf. Sect. 18.7). We have already seen (Sect. 33.5) that this can decrease the central temperature and, therefore, influence the onset of a burning.

In any case, the nuclear cycles tend to develop central regions with increasing density and with heavier elements. We should note, however, that the later nuclear burnings are not capable of stabilizing the star long enough for us to observe many stars in such phases (as is the case with central hydrogen burning and helium burning). The main reason for this is the strongly decreasing difference in binding energy per nucleon (Fig. 18.1). Table 35.1 on page 447 gives typical durations for the various hydrostatic burning phases. From carbon burning on, these are comparable, respectively much shorter than the thermal timescale of the star. This means that any change in the core is no longer reflected by a change of surface properties, and therefore the star remains at its position in the Hertzsprung-Russell diagram. From the outside, one cannot see whether the star is 10,000 years or 10 h before the final core collapse!

35.2 Evolution of the Central Region

The description of the nuclear cycles in Sect. 35.1 has already given a rough outline of the central evolution of a star. We recognize it easily in Fig. 35.2, where the evolution of the centre is plotted in the $\lg \varrho_c$–$\lg T_c$ plane according to evolutionary calculations for different stellar masses M, covering the full range from brown dwarfs to the most massive stars. We see that T_c indeed rises roughly $\sim \varrho_c^{1/3}$ [cf. (35.1)] as long as the central region remains non-degenerate. Of course, the

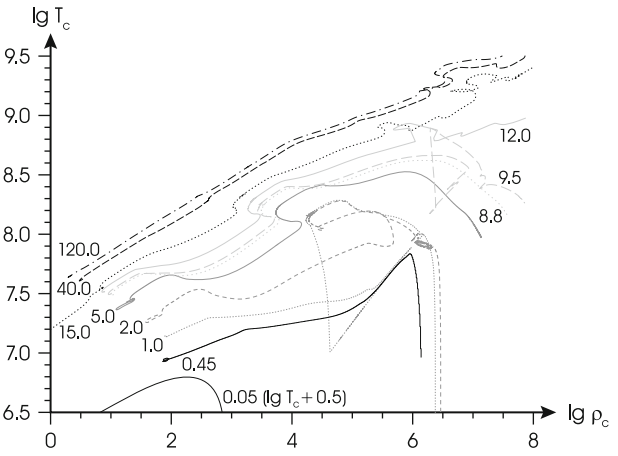

Fig. 35.2 Evolution of the central values of temperature T_c (in K) and density ϱ_c (in $\mathrm{g\,cm^{-3}}$) for stars of all masses (from $0.05 M_\odot$ to $120 M_\odot$). The tracks are labelled with the stellar mass M (in $M_\odot$). The tracks have been collected from different sources but are all for a metallicity of approximately $Z = 0.02$. The brown dwarf track ($M = 0.05\,M_\odot$) includes the pre-main-sequence phase and is from Baraffe et al. (2003). Stars with M from 0.45 to $5\,M_\odot$ are from the authors, those with $M = 8.8$, 9.5, and $12.0\,M_\odot$ (the super-AGB range) from Siess (2006a), and the massive stars ($M = 15$, 40, and $120\,M_\odot$) from Limongi and Chieffi (2006) (Data courtesy of I. Baraffe, M. Limongi, L. Siess)

details of the central evolution are much more complicated than predicted by the simple vector field in Fig. 28.1. During the burnings the curves bulge out to the upper left. This is not surprising, since then the changes are far from homologous [which is assumed in (35.1) and for Fig. 28.1], for example, owing to the restratification from a radiative to a convective core. After these interludes of burning, the evolution returns more or less to the normal slope. A parallel shift of the track from one to the next contraction is to be expected, since the contracting region (the core) will in general have a larger molecular weight, but a smaller mass.

We have already mentioned in Sect. 28.1 and in Sect. 35.1 the important fact that each contraction with $T_c \sim \varrho_c^{1/3}$ brings the centre closer to the regime of electron degeneracy. The degree of non-relativistic degeneracy is constant on the steeper lines $T \sim \varrho^{2/3}$. Once the central region has reached a certain degree of degeneracy (where $\alpha = 3/4$ in the simple model of Sect. 28.1), T_c no longer increases, and the next burning is not reached in this way (if at all), as we have already seen in Fig. 28.2. This happens the earlier in nuclear history, the closer to degeneracy a star has been at the beginning, i.e. the smaller M is (cf. Fig. 35.2). Recall (Sect. 22.2) that with increasing mass, also T_c increases, but ϱ_c decreases (Fig. 22.5). Therefore which nuclear cycle is completed before the star develops a degenerate core depends on the stellar mass M.

If the evolution were to proceed with complete mixing, we would only have to consider homogeneous stars of various M and different compositions, and to see whether their contraction leads to ignition ($M > \widetilde{M}_0$) of a certain burning or to a

degenerate core ($M < \widetilde{M}_0$). These limits for reaching the burning of H, He, and C are $\widetilde{M}_0 \approx 0.08, 0.3$, and $0.8 M_\odot$, respectively.

We know that the evolution lies far from the case of complete mixing, and only the innermost core of a star is processed by nuclear burning. But for sufficiently concentrated cores, the central contraction proceeds independently of the conditions at its boundary, i.e. independently of the non-contracting envelope. Therefore the above values $\widetilde{M}_0$ give roughly the limits for the masses of the corresponding cores.

Standard evolutionary calculations (assuming a typical initial composition, no convective overshooting, and no mass loss) give the following characteristic ranges of M, which we already mentioned earlier. After central hydrogen burning, *low-mass stars* with $M < M_1(\mathrm{He}) \approx 2.3 M_\odot$ develop degenerate He cores. After central helium burning, *intermediate-mass stars* with $M < M_1(\mathrm{CO}) \approx 9 M_\odot$ develop a degenerate CO core. And in *massive stars* with $M > M_1(\mathrm{CO})$ even the CO core remains non-degenerate while contracting for the ignition of the next burning. The precise values of the limiting masses M_1 depend, for example, not only on the assumed initial composition but also on details of the physical effects considered. Another important influence is the downwards penetration of the outer convection zone after central helium burning (in the second dredge-up phase). This lowers the mass of the core and therefore encourages the evolution into stronger degeneracy, i.e. it lowers M_1 (cf. Sect. 34.8). The depth of the second dredge-up depends on the choice of the mixing length parameter and the inclusion of convective overshooting. In Fig. 35.2 we see that the models with $M = 0.05$, 0.45, and 8.8 $M_\odot$ just miss the ignition of H, He, and C, respectively.

After a star has developed a strongly degenerate core it has not necessarily reached the very end of its nuclear history. This is only the case if the shell-source burning cannot sufficiently increase the mass of the degenerate core. However, the next burning is only delayed, and it will be ignited later in a "flash" if the shell source is able to increase the mass of the core to a certain limit M'_c. We have seen in Sect. 33.3 that the critical mass for ignition of helium in a degenerate core is $M'_\mathrm{c}(\mathrm{He}) \approx 0.48 M_\odot$, which agrees with the case shown in Fig. 35.2. The corresponding critical mass of a degenerate CO core is $M'_\mathrm{c}(\mathrm{CO}) \approx 1.4 M_\odot$ as we shall see immediately. Note that these limits are appreciably larger than the corresponding lower limits ($\widetilde{M}_0$) for reaching a burning by non-degenerate contraction, as described above. This indicates the possibility that the evolution depends discontinuously on M around the limits $M_1(\mathrm{He})$ and $M_1(\mathrm{CO})$. For example, stars with $M = M_1(\mathrm{He}) - \Delta M$ ignite helium via a flash in a degenerate core of mass 0.48 $M_\odot$, while stars with $M = M_1(\mathrm{He}) + \Delta M$ can ignite helium burning via core contraction in (nearly) non-degenerate cores of about $0.3 M_\odot$ (cf. the idealized scheme in Fig. 35.3). Here one could imagine a bifurcation at $M = M_1$, where fluctuations would decide into which of the two regimes the star turns. In reality (by which we mean numerical models) the limit is "softened up" (a little bit of degeneracy leading to a baby flash, etc.), as can be seen in Fig. 5.19 of Salaris and Cassisi (2005). Nevertheless, the transition range is narrower than $\approx 0.5\ M_\odot$ between the two regimes.

The ignition of He and C under degenerate conditions in the 1.0 and 8.8 $M_\odot$ stars of Fig. 35.2 first leads to a strong cooling and expansion of the core, followed by a

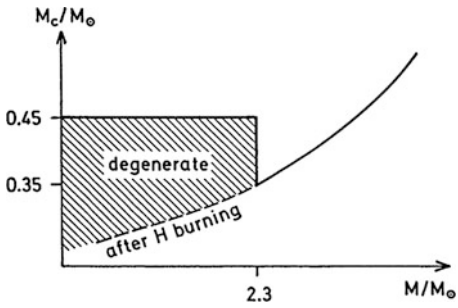

Fig. 35.3 The *solid line* shows schematically the mass M_c of the helium core at the onset of helium burning as a function of the stellar mass M. The *broken line* shows the core mass at the end of hydrogen burning in low-mass stars, before the electron gas in the core becomes degenerate

temperature increase and further expansion until stable core He burning is reached. This realistic evolution is more complicated than the simple picture illustrated in Fig. 33.6.

The evolution of degenerate CO cores is similar to that of degenerate helium cores in low-mass stars (Sects. 33.3 and 33.4). The structure of the core is more or less independent of the details of the envelope. Therefore the evolution of the central values converges for stars of different M as long as the core mass is the same (cf. Fig. 35.2, $M = 0.45$ and $1.0\,M_\odot$). While the mechanical structure of such a core is determined by its mass M_c, its thermal properties depend on the surrounding shell source and on the neutrino losses. If the shell source were extinguished, the core would simply cool down with $\varrho_c =$ constant (on a vertical line in Fig. 35.2) to the white-dwarf state, as can be seen in this figure for the lower and intermediate-mass values. The brown dwarf will end as a hydrogen white dwarf, that with $M = 0.45\,M_\odot$ as a helium white dwarf, those with higher masses up to $8.8\,M_\odot$ as carbon-oxygen white dwarfs, and the one with $9.5\,M_\odot$ possibly as a oxygen-neon white dwarf.

The continuous burning of the shell source increases M_c, which in turn increases the temperature in the shell source (cf. Sect. 33.2). It also increases the central density, as we know from the discussion of the structure of degenerate configurations (Sect. 19.6), i.e. the evolution goes to the right in Fig. 35.2. The contraction due to this effect releases a large amount of gravitational energy, which, in the absence of energy losses (by conduction or neutrinos), would heat the core adiabatically.

However, there are strong neutrino losses ε_ν in this part of the T-ϱ diagram (cf. Fig. 18.11), which modify the whole situation. Since ε_ν increases appreciably with T, we should first make sure that there is no thermal runaway in the degenerate core (a "neutrino flash"), in analogy to a flash at the onset of a burning. This can be easily shown by the stability consideration presented in Chap. 25, where we analysed the reaction of the central region on an assumed increase $d\varepsilon$ of the energy *release*. This led to (25.30) with gravothermal heat capacity c^* (25.29). Now we replace $d\varepsilon$ by the small energy *loss* $-d\varepsilon_\nu$. If we neglect the perturbation of the flux ($dl_s = 0$) for simplicity, (25.29) and (25.30) become

$$c^* \frac{dT}{dt} = -d\varepsilon_\nu, \quad c^* = c_P \left(1 - \nabla_{ad} \frac{4\delta}{4\alpha - 3}\right). \tag{35.2}$$

Obviously the reversal of the sign of the right-hand side in the first equation (35.2) has reversed the conditions for stability. An ideal gas with $\alpha = \delta = 1$ has the gravothermal heat capacity $c^* < 0$, and neutrino losses are unstable since $\dot{T} > 0$ (a thermal runaway with ever increasing neutrino losses). Degenerate cores with $\alpha \to 3/5, \delta \to 0$ have $c^* > 0$, i.e. $\dot{T} < 0$, and these cores are stable: a small additional energy loss reduces T and ε_ν such that the core returns to a stable balance. In the following scheme we summarize the different properties of thermal stability we have encountered:

	Burning ($\varepsilon > 0$)	Neutrinos ($-\varepsilon_\nu < 0$)
Ideal gas	Stable	Unstable
Degeneracy	Unstable	Stable

According to Sect. 34.3 the scheme also holds for burning in shell sources, where we have in addition the pulse instability for thin shells. We recall that a general treatment of the shell source stability is possible (Yoon et al. 2004).

Numerical calculations approve the above conclusions: instead of leading to a thermal runaway, the neutrino losses cool the central region of a degenerate core such that ε_ν remains moderate. Typical "neutrino luminosities" L_ν (= total neutrino energy loss of the star per second) remain only a fraction of the normal "photon luminosity" L. In Fig. 35.4 we show a very instructive example from an early model by Paczyński (1971). Although a star of only 3 $M_\odot$ is almost certainly never able to develop a CO core of more than 0.8 $M_\odot$, the figure still shows all principle effects: The temperature profiles inside the cores of two different M_c are shown in Fig. 35.4 by the broken S-shaped curves. They follow roughly lines of $\varepsilon_\nu =$ constant. With increasing M_c the point for the centre moves along the solid line to the right, and extremely high values of ϱ_c would necessarily occur if M_c could go to the Chandrasekhar limit of $1.44 M_\odot$. Shortly before this limit, at $M_\mathrm{c} \approx 1.4 M_\odot$, the central values reach the dotted line $\varepsilon_\nu = \varepsilon_\mathrm{C}$ to the right of which pycnonuclear carbon burning dominates over the neutrino losses, $\varepsilon_\mathrm{C} > \varepsilon_\nu$. Now carbon burning starts with a thermal runaway. If this happens in the centre, then explosive carbon burning will finally disrupt the whole star, such that one should expect a supernova outburst that does not leave a remnant (a neutron star); compare this also with Chap. 36. We have already seen (Sect. 34.8) that in more massive stars carbon ignition starts in a shell, such that the star survives this event, but the principal story remains that the degenerate CO core is ignited when its mass $M_\mathrm{c} \approx 1.4 M_\odot$, although it depends on the initial mass and varies, according to Siess (2006b), between 1.1 and 1.5 $M_\odot$ for ZAMS masses between 9.0 and 11.5 $M_\odot$. With increasing mass and decreasing core degeneracy the location of carbon ignition is moving towards the centre. At the end of the rather complicated carbon burning phase an ONeMg core is left over. For the initial mass range for which this core is degenerate, its mass is between 1.05 and 1.12 $M_\odot$, again far from the Chandrasekhar mass.

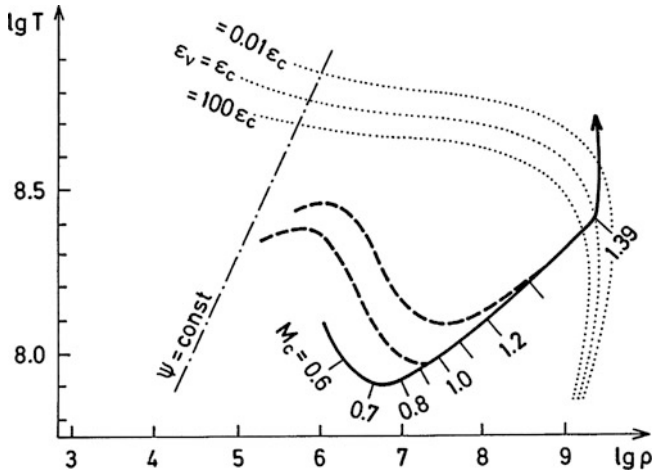

Fig. 35.4 Temperature T (in K) and density ϱ (in g cm^{-3}) in the CO core of a $3M_\odot$ star after central helium burning. The *solid line* gives the evolution of the centre with increasing core mass M_c (in $M_\odot$). The carbon flash starts at about $M_c = 1.39M_\odot$ when the energy production by carbon burning (ε_C) exceeds the neutrino losses (ε_ν). Some lines of constant ratio $\varepsilon_\nu/\varepsilon_C$ are *dotted*. The *broken lines* show the T stratification in the core for two consecutive stages; neutrino losses have produced a maximum of the temperature outside the centre (After Paczyński 1971)

The just-described central evolution is the same for all stars that are able to develop a degenerate CO core of $M_c \approx 1.4M_\odot$. The obvious condition for this is that the stellar mass M is larger than that limit. For $\dot{M} = 0$ this would include all stars in the range $1.4M_\odot < M < 9M_\odot$, i.e. the intermediate-mass stars ($M \approx 2.3 \ldots 9M_\odot$) and the low-mass stars with $M > 1.4M_\odot$. More precisely the stellar mass M must be larger than $1.4M_\odot$ *at the moment of ignition* (which does not occur before $M_c \approx 1.4M_\odot$). This can require that the initial stellar mass M_i (on the main sequence) was much larger than $1.4M_\odot$ if M has been reduced in the meantime by a strong mass loss.

Obviously there are two competing effects, the increase of M_c due to shell-source burning and the simultaneous decrease of the stellar mass M due to mass loss. Their changes in time are schematically shown in Fig. 35.5, and the outcome of this race decides the final stage of the star. The two values (M and M_c) reach their goal at $1.4M_\odot$ simultaneously if the initial mass has the critical value $M_i(\min)$. Stars with $M_i > M_i(\min)$ will ignite the CO core, since M_c can reach $1.4M_\odot$. For stars with initial masses $M_i < M_i(\min)$, the mass loss will win and M_c never reaches $1.4M_\odot$. Such stars will finally cool down to the white-dwarf state after the shell source has died out near the surface (cf. Sect. 33.7). Unfortunately the total loss of mass during the evolution is not well known. The various mass loss formulae (Sect. 32.3) and the initial-final mass relation (Fig. 34.7) predict a total mass loss of up to $\Delta M \approx 6 \ldots 7\, M_\odot$, which would mean a critical initial mass above $M_i(\min) \approx 7\, M_\odot$ at least. Of course, if the mass loss were so large that even stars

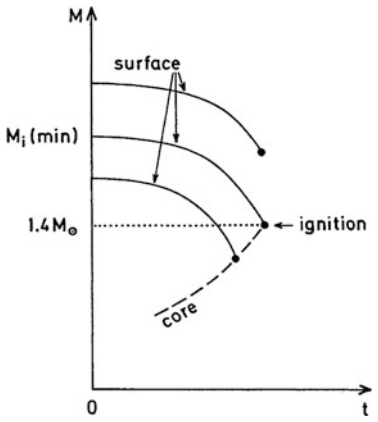

Fig. 35.5 For three different initial masses M_i the *solid lines* show schematically the decrease of the stellar mass M due to mass loss, while the mass of their degenerate CO cores (*dashed line*) increases owing to helium-shell burning. Carbon burning is ignited when the core mass reaches about $1.4 M_\odot$. This never occurs for $M_i < M_i(\text{min})$, since then the surface reaches the core before it can grow to $1.4\ M_\odot$

Table 35.1 The duration of burning stages (in years) in three models of different mass, taken from Limongi and Chieffi (2006)

Burning:	$M = 15\ M_\odot$:	$M = 40\ M_\odot$:	$M = 120\ M_\odot$:
H	1.31×10^7	4.88×10^6	2.80×10^6
He	9.27×10^5	3.82×10^5	2.96×10^5
C	3.25×10^3	1.86×10^2	3.62×10^1
Ne	6.67×10^{-1}	1.34×10^{-1}	6.56×10^{-2}
O	3.59×10^0	1.59×10^{-1}	2.57×10^{-2}
Si	6.65×10^{-2}	1.47×10^{-3}	3.63×10^{-4}

The beginning and end of each burning stage is defined as the times when 1 % of the fuel has been burnt, respectively when its abundance has dropped to below 10^{-3} (Data courtesy M. Limongi)

with $M_i \approx 10\ M_\odot$ were reduced to $M < 1.4\ M_\odot$ before carbon ignition, then all intermediate stars (developing a degenerate CO core) would become white dwarfs. In any case, there are drastic differences between the final stages (white dwarfs or explosions) to be expected for stars in a narrow range of M_i near $M_i(\text{min})$. Current models (Sect. 34.8 and Fig. 35.2) put this mass range between ≈9 and 11 $M_\odot$. These numbers are all depending on the composition.

It is clear that we have the same competition between $\dot{M}_c > 0$ and $\dot{M} < 0$ in the analogous problem of determining initial masses for which the degenerate helium cores are ignited (at $M_c \approx 0.48\ M_\odot$). In this case the bifurcation of the evolution concerns mainly the composition of the final white dwarfs (He or CO).

Finally, we have to consider the massive stars with $M > 9 \ldots 11\ M_\odot$, in which the CO core does not become degenerate during the contraction after central helium burning. Therefore T_c rises sufficiently during this contraction to start the (non-explosive) carbon burning. Here the neutrino losses can become very large, carrying away most of the energy released by carbon burning. In the later burnings, massive stars can have neutrino luminosities up to 10^6 times larger than L; but these stages are very short-lived: for example, silicon burning lasts just a few days (see Table 35.1).

These massive stars will go all the way through the nuclear burnings until Fe and Ni are produced in their central core (Such a case is illustrated in the onion skin model in Fig. 35.1.). After the core has become unstable and collapses, electron captures by these nuclei transform the core into a neutron star, while the envelope is blown away by a supernova explosion (see Chap. 36).